ACTIVITY OF MUSCLE AND PAW-SKIN AFFERENTS DURING CAT LOCOMOTION COMPUTED USING A FORWARD DYNAMICS NEUROMECHANICAL MODEL

[1]Boris I. Prilutsky, [1]Alexander N. Klishko, [2]Douglas J. Weber, [3]Michel A. Lemay
[1]School of Applied Physiology, Center for Human Movement Studies, Georgia Institute of Technology, Atlanta, USA
[2]Departm. of Physical Medicine and Rehabilitation and Departm. of Bioengineering, University of Pittsburgh, Pittsburgh, USA
[3]Department of Neurobiology and Anatomy, Drexel University College of Medicine, Philadelphia, USA
Email: boris.prilutsky@ap.gatech.edu, web: http://www.ap.gatech.edu/Prilutsky/

SUMMARY
The structure and function of the mammalian locomotor central pattern generator (CPG) and its control by afferent feedback *in vivo* are not completely understood due to experimental limitations. Our long-term goal has been to develop a comprehensive neuromechanical model of the spinal control of locomotion by combining a CPG model with a musculoskeletal model of cat hindlimbs generating realistic motion-dependent afferent signals. The aim of this study was to develop a forward dynamics model of cat hindlimbs that uses neural or muscle activity as input and generates realistic locomotion and somatosensory feedback signals. A planar, forward dynamics, 10-DOF model of two hindlimbs, pelvis and trunk driven by 18 Hill-type muscle actuators was developed. Generated model motion and simplified regression equations relating computed mechanical variables with the firing rates of muscle afferents allowed for computing type Ia, Ib, II muscle and paw pad-skin afferent activity. Patterns of muscle activity, muscle fascicle length changes and hindlimbs' motion recorded during walking of five cats were used for obtaining model input and identifying model parameters. The model demonstrated a close match between computed and recorded walking mechanics and activity of selected afferents. The computed feedback signals were consistent with their suggested role in triggering locomotor phase transitions.

INTRODUCTION
A network of neural circuits in the lumbar region of the mammalian spinal cord, called central pattern generator (CPG), can produce hindlimb locomotor activity even without descending commands or motion-dependent proprioceptive feedback [1]. The CPG rhythmic activity *in vivo* is modulated by supraspinal commands [10] and afferent feedback [11], however the mechanisms of afferent CPG regulation in mammals are still elusive due to experimental difficulties in recording from spinal neurons in moving animals. Neuromechanical modeling and computer simulations may help to address this problem. Several models of terrestrial locomotor CPGs integrated with biomechanical systems through motion-dependent feedback have been developed and analyzed, e.g. [3,8]. In most of these studies, however, either the CPG model did not reproduce the relevant experimental observations (e.g., CPG responses to afferent nerve stimulations [14]) or the musculoskeletal models were oversimplified. Our long-term goal is to develop a comprehensive neuromechanical model of mammalian locomotor system that integrates a CPG model, reproducing fictive locomotion experiments [14], with a detailed musculoskeletal model of the cat hindlimbs that reproduces walking mechanics and limb afferent signals. The aims of this study were (1) Develop a forward dynamics model of cat hindlimbs that generates the activity of spindle (Ia, II), tendon organ (Ib), and paw pad cutaneous afferents using recorded muscle activity and computed muscle fiber length, velocity and forces; (2) Compare computed muscle length- and force-dependent afferent signals with activity of selected afferents recorded during cat locomotion [5,6,13,15] and (3) Examine if computed proprioceptive signals were consistent with their suggested role in triggering locomotor phase transitions [10,11].

METHODS
All experimental procedures in this study were approved by the Institutional Animal Care and Use Committee of Georgia Institute of Technology. The cat hindlimbs with the pelvis and trunk were modeled as a 10-DOF sagittal plane system of rigid segments interconnected by frictionless revolute joints (Figure 1A,B). Interactions of the hindlimbs with the external environment were modeled by linear springs and dampers. The equations of limb dynamics included the generalized body segment accelerations and velocities, Coriolis, centripetal, gravitational, ground reaction and muscle forces [3]. The hindlimbs were driven by 18 Hill-type muscle actuators (Figure 1C) whose contraction dynamics description included muscle mass, pennation angle and force-length-velocity properties of muscle and tendon, e.g. [16]). The firing rates of muscle Ia and II spindle afferents were calculated as functions of muscle fascicle length, velocity and EMG activity using modified regression equations developed by [13]. To compute the firing rate of Ib Golgi tendon afferents, we assumed the Ib activity being proportional to muscle force during the mid-range of forces, e.g. [2,4]. The firing rate of cutaneous afferents from the plantar surface of the paw was calculated as a function of the vertical ground reaction and the positive rate of its change. The equations of hindlimb and muscle dynamics were integrated numerically over a complete walking cycle by a 2-nd order Runge-Kutta method (0.02-ms time step). Rectified and low-pass filtered EMG patterns of 9 hindlimb muscles, fascicle length of selected muscles and the initial coordinates and velocities of the hindlimb segments were recorded in 5 adult cats (as described in [7,9,12]) and used as input to the model. Activity of paw pad afferents was recorded using implanted chronic electrodes in the dorsal root ganglion of a select cat (as described in [15]). A simulated annealing optimization algorithm was used to find model parameters that minimized mismatch between computed and experimentally obtained joint angles, joint moments and ground reaction forces.

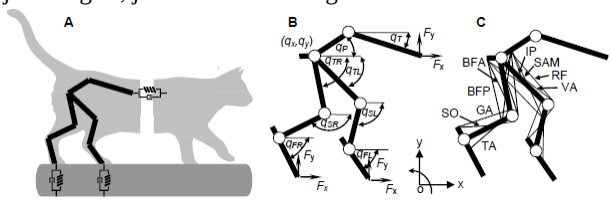

Figure 1: A, B: 10-DOF model of hindlimbs and trunk. C: 18 Hill-type muscle actuators driving the model.

RESULTS AND DISCUSSION
Identified model parameters allowed for a close match (typically within ±1SD) between simulated and recorded

walking mechanics (Figure 2). The comparison of computed and recorded activity for biceps femoris posterior (BFP),

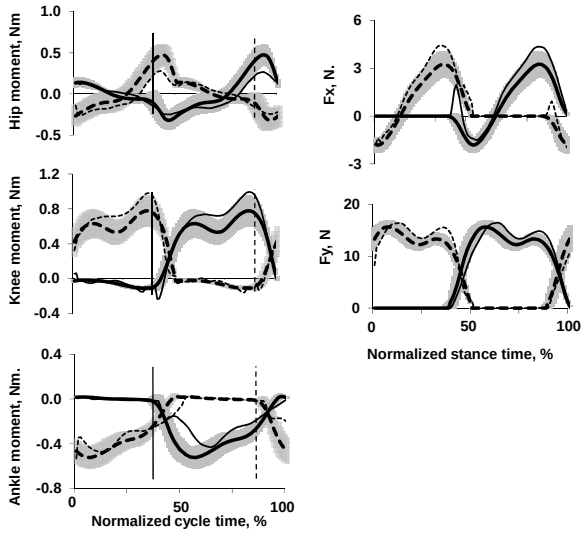

Figure 2: Recorded mean (thick lines) ± SD (gray shadow) and computed (thin lines) joint moments (left panel) and anterior-posterior Fx and vertical Fy ground reaction forces (right panel) of two hindlimbs during a cycle of walking. The continuous lines correspond to the left hindlimb and the dashed lines correspond to the right hindlimb. The continuous and dashed vertical lines in left panel indicate paw contact with the ground by the left and right hindlimb, respectively. Positive moments are flexor for the ankle and hip and extensor for the knee. The experimental mean and SD values for the mechanical variables were obtained from 5 cats.

vastii (VA) and triceps surae (soleus, SO and gastrocnemii, GA) afferents showed reasonable qualitative agreement (Figure 3). Specifically, the computed and recorded type Ia and II BFP afferents had peak activity near paw contact (Figure 3A,B). The computed and recorded GA and SO Ib afferents were mostly active during stance, whereas BFP Ib activity occurred at the stance-swing and swing-stance transitions (Figure 3C). The computed instantaneous firing rate of cutaneous paw pad afferents demonstrated a sharp peak at paw contact and a moderate magnitude during the rest of stance, similar to the recorded activity of mechanoreceptors from paw pad (Figure 3D).

Computed afferent activity suggest that type II afferents from hip flexors (not shown) may trigger the CPG extension (stance)-flexion (swing) phase transition as their activity peaks at terminal stance, while load sensitive extensor muscle Ib and cutaneous paw afferents have low activity at that time. These findings are consistent with earlier similar suggestions [11]. Type Ia and II afferents from BFP could participate in controlling the flexion-extension (or swing-stance) phase transition since these afferents reach their maximum activity at terminal swing (Figure 3 A,B).

CONCLUSIONS

Given the reasonable agreement between computed and recorded activity of type Ia, Ib and II afferents from selected muscles, as well as of paw pad afferents, the developed model can now be integrated with the CPG model by [14] and used for a closed-loop simulations and computational studies of spinal locomotion. These simulations have the potential to provide additional information compared to previous similar simulations [3,8] because the CPG model [14] and the musculoskeletal model developed in this study reproduce well the activity patterns during fictive locomotion [10,14] as well as the mechanics (Figure 2) and afferent activity (Figure 3) during real cat locomotion.

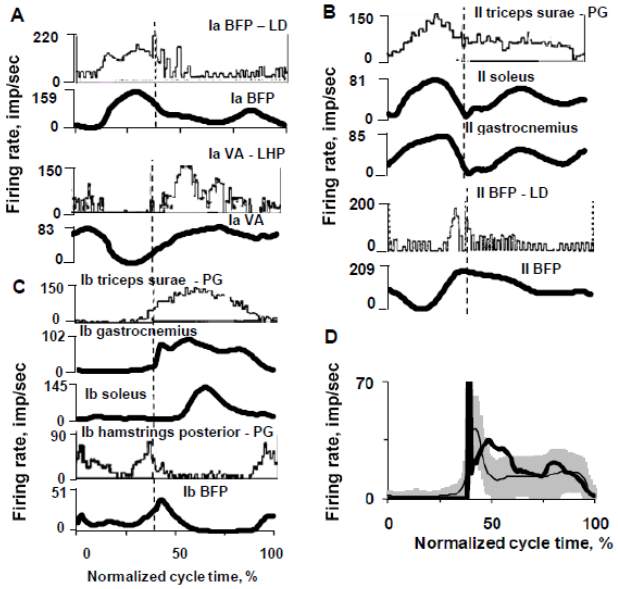

Figure 3: Comparison of computed (black thick lines) and recorded *in vivo* (gray thin lines) firing rates of group Ia (A), II (B) and Ib (C) afferents from selected muscles and cutaneous paw pad afferents (D). The vertical dashed lines separate the swing and stance phases. Muscle abbreviations are the same as in the text. *In vivo* activity of muscle afferents are reproduced with permission from: Ia BFP – LD and II BFP – LD, Figure 2 in [5]; Ia VA – LHP, Figure 3 in [6], II triceps surae – PG, Ib triceps surae – PG and Ib hamstrings posterior - PG, Figure 6 in [13]. The mean (thin line)± SD (gray shadow) activity of paw pad afferents in D is obtained from recorded 4 afferents of one animal collected during 11 cycles.

ACKNOWLEDGEMENTS

The study was supported by NIH grants NS-048844 and EB 012855 and by the Center for Human Movement Studies at Georgia Institute of Technology.

REFERENCES

1. Brown TG, *J Physiol*, **48**:18-46, 1914.
2. Crago PE et al., *J Neurophysiol*, 47, 1069-1083, 1982.
3. Ivashko et al., *Neurocomputing*, **52-54**:621-629, 2003.
4. Houk et al., *J Neurophysiol*, **46**:143-166, 1981.
5. Loeb GE, Duysens J, *J Neurophysiol*, **42**:420-440, 1979.
6. Loeb, GE et al., *J Neurophysiol*, **54**:549-564, 1985.
7. Maas et al., *J Appl Physiol*, **106**:1169-1180, 2009.
8. Markin et al., *Ann N Y Acad Sci*, **1198**:21-34, 2010.
9. Markin et al., *J Neurophys*, **107**:2057-2071, 2012.
10. McCrea DA, *J Physiol*, **533**:41-50, 2001.
11. Pearson KG, *Brain Res Rev*, 57, 222-227, 2008.
12. Prilutsky et al., *J Neurophys*, **94**:2959-2969, 2005.
13. Prochazka A, & Gorassini M, *J Physiol*, **507**:293-304, 1998.
14. Rybak IA, et al., *J Physiol*, **577**:641-658, 2006.
15. Weber et al., *J Neural Eng*, **4**:S168-S180, 2007.
16. Zatsiorsky VM, Prilutsky BI, *Biomechanics of Skeletal Muscles*. Human Kinetics, 2012.